

Network Sensitivity of Systemic Risk

Domenico Di Gangi¹, D. Ruggiero Lo Sardo^{2,3}, Valentina Macchiati⁴, Tuan Pham Minh^{2,3},
Francesco Pinotti⁵, Amanah Ramadiah⁶, Mateusz Wilinski^{1,*} and Giulio Cimini^{7,8}

¹*Scuola Normale Superiore, Piazza dei Cavalieri 7, 56126 Pisa, Italy*

²*Complexity Science Hub Vienna, Josefstädterstrasse 39, 1080, Vienna, Austria*

³*Section for the Science of Complex Systems, CeMSIIS,
Medical University of Vienna, Spitalgasse 23, 1090 Vienna, Austria*

⁴*Department of Physics, University of Turin,
Via Pietro Giuria 1, 10125 Torino, Italy*

⁵*EPIcx Lab, INSERM, Faculty of Medicine, Sorbonne University,
iPLESP UMR-S 1136, 27 rue Chaligny, 75015 Paris, France*

⁶*Department of Computer Science, University College London, London WC1E 6BT, United Kingdom*

⁷*IMT School for Advanced Studies, Piazza Sann Francesco 19, 55100 Lucca, Italy and*

⁸*Institute for Complex Systems (CNR), via dei Taurini 19, 00185 Roma, Italy*

The recent stream of literature of systemic risk in financial markets emphasized the key importance of considering the complex interconnections among financial institutions. Much effort has been put to model the contagion dynamics of financial shocks, and to assess the resilience of specific financial markets—either using real data, reconstruction techniques or simple toy networks. Here we address the more general problem of how the shock propagation dynamics depends on the topological details of the underlying network. To this end, we consider different network topologies, all consistent with balance sheets information obtained from real data on financial institutions. In particular, we consider networks with varying density and mesoscale structures, and vary as well the details of the shock propagation dynamics. We show that the systemic risk properties of a financial network are extremely sensitive to its network features. Our results can thus aid in the design of regulatory policies to improve the robustness of financial markets.

I. INTRODUCTION

The several crises that happened in the last two decades lead scientists and regulators to rethink the approach used to assess market risk with a systemic perspective [1–7]. A common denominator that emerged from these works is the importance of considering the structure of financial dependencies [8–12], a thing that pushed the research in the direction of designing novel systemic risk mechanisms [13]—from the seminal approaches of Eisenberg & Noe [14] and Furfine [15] to the recently introduced DebtRank centrality [16]. These methods are nowadays implemented in stress tests performed by central banks [17], and the current scientific challenge is thus no longer to quantify the systemic risk but to suggest specific regulatory solutions to change the structure of the system in order to diminish risk. To this end, it is essential to understand which features of a financial network make it more or less resilient to systemic risk. In this work we focus precisely on this challenge.

One of the first works in this direction is that of Gai & Kapadia [2], where it was shown that random Poisson networks are “robust-yet-fragile”: and the probability of contagion is maximal for intermediate network density, whereas systemic losses monotonically increase with the network connectivity. Mastromatteo et al. [18] further show that, under the Furfine dynamics, sparse Poisson networks in general lead to more defaults than very dense networks. Roukny et al. [19]

*Electronic address: mateusz.wilinski@fuw.edu.pl

showed that no single topology always leads to the lowest risk (in particular, scale-free networks can be both more robust and more fragile than homogeneous Poisson architectures). Leon & Berndsen [20] argue that modular scale-free architectures favor robustness, whereas, Montagna & Lux [21] show that the dependence of systemic risk on the density changes if shocks are correlated. Bardoscia et al. [22] show that, under the DebtRank dynamics, the system's stability decreases with the density due to the presence of cycles.

In this work we aim to set an exploration of the network sensitivity of systemic risk which encompasses these previous findings, and extends them by considering modular, core-periphery and bipartite network structures.

II. METHODOLOGY

A. Data

To build financial (interbank) networks, we use the Bankscope dataset [23] containing the balance sheet of the 100 largest European banks. In particular, we have information about the interbank assets A_i , the interbank liabilities L_i and the equities E_i of each i of these banks, and we consider data for years 2008 and 2013 (i.e, before and after the global financial crisis) [24]. We recall that the equity of a bank is the difference between its positive positions and its obligations to creditors. When the equity is positive the bank is solvent, otherwise it goes bankrupt (defaults) because it would not be able to refund its debts. Since the chosen group of banks is not an isolated systems, interbank assets and liabilities do not sum up to the same value; in order to have a closed system, we rescale them to have $\sum_j A_j = \sum_j L_j$.

B. Network Generation

In the literature on financial networks, interbank markets are typically reconstructed from balance sheet data—before being tested for systemic risk [25]. Here we use and generalize the approach of Cimini et al. [26] to generate (rather than reconstruct) financial networks compatible with balance sheet information. The method is based on a combination of Exponential Random Graphs [27, 28] and the fitness model [29] (see further details in [26, 30]).

First, we generate an unweighted directed graph by drawing each edge $i \rightarrow j$ independently with probability:

$$p_{i \rightarrow j} = \frac{z A_i L_j}{1 + z A_i L_j}, \quad (1)$$

where $z \in (0, \infty)$ is a parameter controlling for the density of the network. Indeed, since the values of assets and liabilities are given, this probability is an increasing function of z , hence the link density of the network is proportional to the parameter z . We consider also the possibility of having self-loops in the graph because some of the top European banks may represent banking group with internal flow of money. The alternative possibility would be to use the RAS algorithm to get rid of self loops [31].

We then assign a weight to each link, in accordance with the generated graph adjacency matrix $a_{i \rightarrow j}$, as follow:

$$w_{i \rightarrow j} = \frac{A_i L_j}{W p_{i \rightarrow j}} a_{i \rightarrow j} \quad (2)$$

where $W = \sqrt{(\sum_i A_i) (\sum_j L_j)}$. The final result is a weighted directed network given by the corresponding adjacency matrix A whose entries are $A_{ij} = w_{i \rightarrow j}$. In the economic network literature this matrix is referred to as the asset matrix while its transpose is called the liability matrix.

The distribution of assets and liabilities across banks is heterogeneous, and with such an input our network construction method generates a core-periphery, independently on the network density. In order to get rid of this constraint, we introduce a generalization of Eq. 1.

$$p_{i \rightarrow j} = \frac{z (A_i L_j)^\phi}{1 + z (A_i L_j)^\phi}, \quad \phi \in [0, 1]. \quad (3)$$

The new parameter ϕ allows to model a wide range of network topologies (for fixed z), including the fitness-induced configuration model and the Erdos-Renyi random graphs as the two limits ($\phi = 1$ and $\phi = 0$, respectively).

C. Block Structure

The network generation method allows one to explore different network structures. Thus one can further decompose the adjacency matrix A into blocks. Here, for the sake of simplicity, we shall restrict our consideration to the case in which there are only four blocks present in A as following

$$A = \begin{pmatrix} A_{11} & A_{12} \\ A_{21} & A_{22} \end{pmatrix}$$

Each block A_{nm} , $n, m = \overline{1, 2}$ represents a subgraph of the network in which the link density is characterized by z_{nm} , $n, m = \overline{1, 2}$. Furthermore, among all possible topological configurations, there are three distinct ones that we shall focus on, namely the modular, the core-periphery and the bipartite-like structures.

a) The modular topology

In this case the network is clustered into two groups of nodes with dense connections within the groups and sparse connections between them. The configuration corresponds to the choice of z_{11} and z_{22} such that they are both much larger than z_{12} and z_{21} . In the implementation, this can be achieved in a following manner: without loss of generality, put $z_{12} = z_{21} = z$, $z_{11} = z_{22} = \lambda z$ and then generating the blocks A_{11} and A_{22} with λz and those A_{12} and A_{21} with z , where $\lambda \in [0, 1]$.

b) The bipartite-like topology

As an opposing configuration of the modular structure, one can consider the case in which the interconnections between the two communities dominate over the connections inside each community. The parameterization now is given by $z_{12} = z_{21} = \lambda z$ and $z_{11} = z_{22} = z$, where $\lambda \in [0, 1]$.

c) The core-periphery topology

Of special interest in the investigation of financial networks is the case in which a core-periphery relationship between two groups of banks is observed. This situation results in a higher link density in the first group while it is lower in the second one. As mentioned in the last section, the network generated by Eq. (1) inherently possesses the core-periphery structure. Therefore, any parameterization of the form $z_{12} = z_{21} = \gamma z$, $z_{22} = \gamma^2 z$ and $z_{11} = z$, where $\gamma \in [0, 1]$, would show only small differences between the two extreme $\gamma = 0$ and $\gamma = 1$. This is why we need to use the Eq. (3) to generate the core-periphery topology.

D. DebtRank

Once the network is constructed, we use the DebtRank to model the propagation of shocks in a network of banks [32, 33]. We consider the relative loss of equity $h_i(t)$ for bank i and the interbank leverage matrix $\Lambda_{ij}(t)$:

$$h_i(t) = \frac{E_i(0) - E_i(t)}{E_i(0)} \quad (4)$$

$$\Lambda_{ij}(t) = \begin{cases} \frac{A_{ij}(0)}{E_i(0)} & \text{if bank } j \text{ has not defaulted up to time } (t-1) \\ 0 & \text{otherwise} \end{cases} \quad (5)$$

The dynamical equation for the relative equity $h_i(t)$ reads:

$$h_i(t+1) = \min \left[1, h_i(t) + \sum_{j=1}^N \Lambda_{ij}(t) [p_j^D(t+1) - p_j^D(t)] \right] \quad (6)$$

where $p_j^D(t) = h_j(t)e^{\alpha[h_j(t)-1]}$ is the probability of default of bank j at time t , and $\alpha \in (0, \infty)$ is a controlling parameter which allows to switch continuously from the linear DebtRank ($\alpha = 0$) [32] to the Furfine algorithm ($\alpha \rightarrow \infty$) [15].

We define the average equity loss as the quantity:

$$\bar{E}_{loss} = \sum_i \frac{[h_i(t) - h_i(1)]E_i(0)}{\sum_i E_i(0)} \quad (7)$$

where $E_i(0)$ is the initial equity of the bank i , and $h_i(1)$ is the initial shock on equity for i .

We use two kind of stopping criteria during the simulation: when the difference $cond = \|(h(t) - h(t-1))E(0)\|_2$ becomes smaller than a tolerance tol , or when the number of interactions is equal to max_{iter} . The value of the parameters tol and max_{iter} depends on the studied cases.

III. RESULTS

We reconstruct the interbank network for year 2008 and 2013. We then run the stress test according to DebtRank shock propagation mechanism on the reconstructed network. Finally, we measure the \bar{E}_{loss} of all banks. We do this over different network density ρ . For each ρ , we sample 10 networks and calculate the average \bar{E}_{loss} over these networks. In term of initial shock, we do the uniform shock by reducing the equity value of each bank by θ of its initial equity. Figure 1 shows the result of this exercise for ρ ranges from 0 to 1, and θ ranges from 0 to 0.6.

First, we see from the figure that the \bar{E}_{loss} increases as the ρ increases. This implies that the network becomes more fragile when it becomes more dense. Second, we find a significant \bar{E}_{loss} value for the small θ in the 2008 data. However, we see that \bar{E}_{loss} decreases as the ρ gets larger. This implies that there is a critical value of θ where the sufficiently small shock propagates to the entire network and causes almost all the banks to default. From the figure, we see that the critical value is around 0.1 for the 2008 data. Finally, by comparing the 2008 data and the 2013 data, we find that the \bar{E}_{loss} for every combination of ρ and θ has changed significantly from before the 2008 crisis to after the crisis. The figure shows that the network of the 2013 data is more robust compare to the network of the 2008 data.

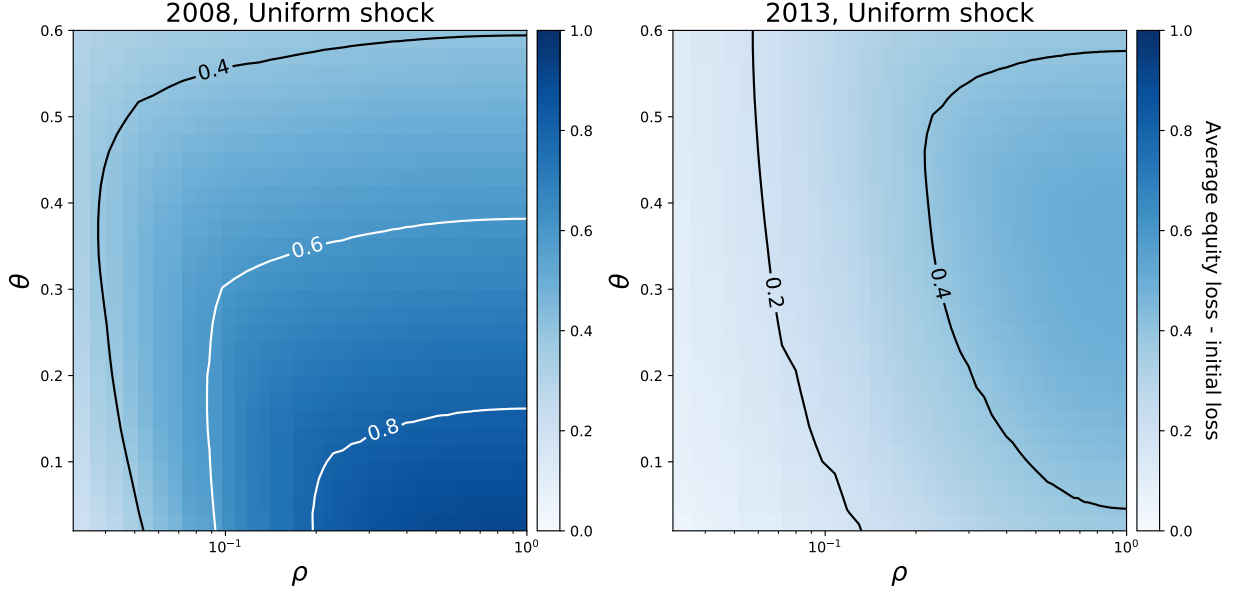


FIG. 1: \overline{E}_{loss} as a function of the link density and the magnitude of the uniform shock for the 2008 (left) and the 2013 data (right). Darker (brighter) color refers to the higher (smaller) DebtRank, which corresponds to a more fragile (resilient) financial network.

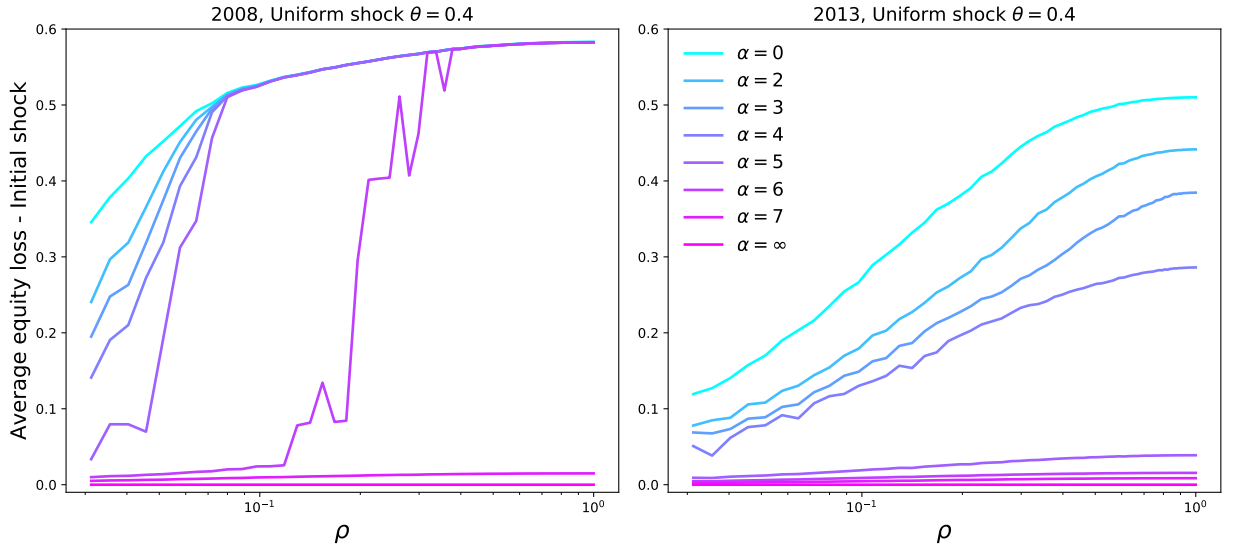


FIG. 2: \overline{E}_{loss} as a function of the link density for a fixed value of initial shock, $\theta = 0.4$ uniform shock in the 2008 case (left) and the 2013 data (right). Different curves correspond to different magnitudes of non-linearity in the relation between DebtRank and average equity loss.

Previously, we have looked at the case of the DebtRank. This is the case where $\alpha = 0$ in the Equation 7. Here we do the similar exercise, but we look at for different value of α . In particular, we are interested in the case DebtRank, Furfine, and the non-linear model in between. To this end, we look at the value of $\alpha = 0, 2, 3, 4, 5, 6, 7, \infty$. Figure 2 shows the results for this exercise.

First, we look at the case for the network of 2008 data. Here we find that, in respect to ρ , the \overline{E}_{loss} increases and converges towards a possible highest value of \overline{E}_{loss} . In contrast, we see a

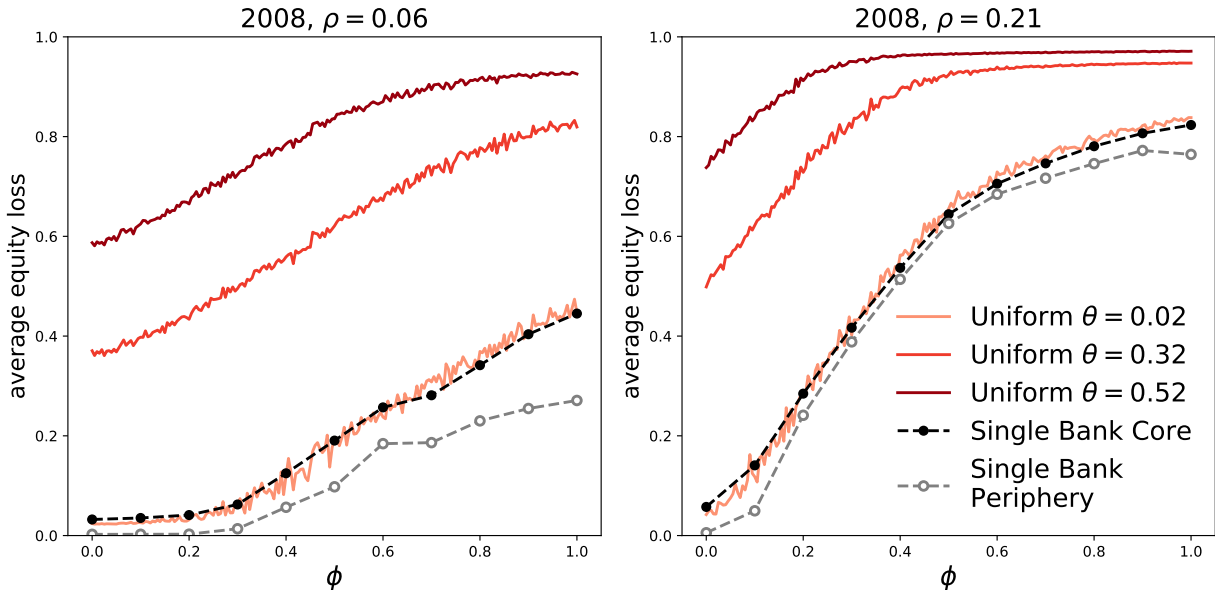


FIG. 3: \overline{E}_{loss}^* as a function of the parameter ϕ tuning core-periphery structure in the 2008 interbank network case for $\rho = 0.06$ (left) and $\rho = 0.21$ (right). Full lines correspond to a uniform shock protocol.

different behavior of \overline{E}_{loss} for the large α . We also find a completely different behavior of \overline{E}_{loss} for the case of $\alpha = 0.5$. Here we find that it shows a similar behavior to the case of large α in the regime of small ρ , but instead it shows a similar behavior to the case of small α in the regime of large ρ .

The behavior we describe above is not seen for the case of 2013 data. Here we find instead that \overline{E}_{loss} for different α never converge towards similar value.

Up to this point, we have looked at the case of $\phi = 1$ where we use the fitness configuration model to reconstruct the interbank network. Here we look at the case of other value of ϕ . In principle, we are interested to look at the effect of different topological properties on the value \overline{E}_{loss} value. To do this, we do the similar exercise as above, but we tune the parameter ϕ this time. Figure 3 shows the result from this exercise.

First, we see from the figure that the \overline{E}_{loss}^* increases as the ϕ increases. This means that the network with core-periphery structure shows more fragile behavior towards the shock. By looking at the figure for the case of $\rho = 0.06$ and $\rho = 0.21$, we see that this behavior is consistent for both density. Additionally, we also find that as the density increases, the difference of \overline{E}_{loss}^* for each ϕ also increases.

To look at the \overline{E}_{loss}^* in other topological properties, here we do the above exercise but for the communities topology network. We shock the first community, and measure the \overline{E}_{loss}^* of the second community. Finally, we look at the bipartite topological structure. Figure ?? shows the result for these exercises. Here we see that as the initial shock increases, the network becomes more fragile, for both the communities topological structure and the bipartite topological structure.

IV. DISCUSSION

We have examined different topological properties and shown how they affect the systemic risk. In addition, we also used variety of shock types and changed the way they propagated across the network. The results prove how complex the interbank system is and how many variables are

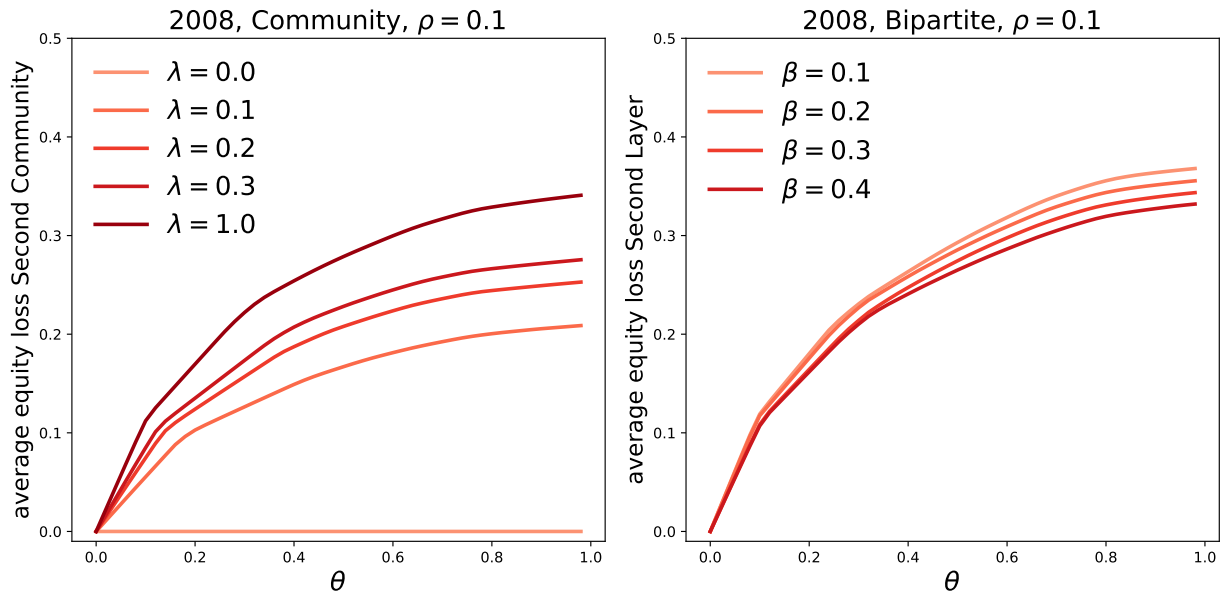


FIG. 4: \bar{E}_{loss}^* as a function of the parameter θ in the 2008 interbank network case for the communities topological structure (left) and the bipartite topological structure (right). The $\rho = 0.1$ is used.

involved in shaping its resilience.

For the simplest situation of Eq. (3) when $\phi = 1$, and it reduces to Eq. (1), there is a qualitative difference between the behavior observed in 2008 and 2013. As shown in figure 1, the crisis shaped the interbank market in a way that it is much more robust to small shocks even in the high density regime. But the change of systemic properties of the system is more significant. To describe it, we will need to look at the figure 2. Different values of the parameter α can be seen as different approaches of the market participants towards losses in their counterparts equity. The higher the α , the higher the confidence in the counterpart ability to recover from losses. In 2008 we observed two significant regimes of the propagation, depending on the network density and the parameter α . If the confidence in the system was not high enough, at some given density, the system jumped to a contagion state, equal to the one observed for $\alpha = 0$. On the other hand, in 2013, even for low confidence, increasing the density did not result in an asymptotic value equal to the one observed in the no-trust case.

Above results are interesting from the perspective of crisis impact but they also imply that different structure of balance sheet changes the way the system reacts to various topological properties. We would like to explore this direction in the future work by repeating the simulations for different synthetic balance sheet structures.

It should also be pointed out that across different α we observed increasing risk as a function of density. This was, however, obtained with uniform shock in all equities. As shown in [18], if we consider defaulting single bank, we expect increasing density to help the system withstand the shock, at least for $\alpha = 1$.

The method of network reconstruction described by Eq. (1) imposes, as a result of fat tail distribution of assets and liabilities, a core-periphery structure. As a consequence, the only topological parameter used before, was the network density. By introducing parameter ϕ in Eq. (3) we were able to continuously change the network structure from a random one ($\phi = 0$) to a core-periphery one ($\phi = 1$). As shown in figure 3 the core periphery structure is less resilient, even in the case of point default. It confirms the well known fact that strongly connected nodes increase the shock

propagation. Interestingly, even a shock imposed on the periphery nodes on average propagates faster in the core-periphery structure, compared to homogeneous degree case. This result is similar in both 2008 and 2013, the only difference being the curve slope, which is lower in 2013, confirming the increased post-crisis stability.

In the last step of our analysis we looked at a block structure of a network. In the case of community structure, this can be seen as a study of shock propagation between two connected markets, which may represent different countries. On the other hand, the bipartite case is a simple approximation of a bow-tie structure, which is often observed among financial networks. In both cases we were interested to see how does a shock on one side propagates to the other. The results are presented in the figure ref[]. For communities we can see that the impact has a square-root dependence on the initial shock size. Moreover, in accordance to the intuition, this effect is weaker with decreasing connectivity between the communities. When we move to bipartite the dependence is similar, however it is decreasing when we move further from the bipartite structure. For a constant density, this is an effect of the increasing probability of a connection between two big institutions from different groups.

Acknowledgments: This work is the output of the Complexity72h workshop, held at IMT School in Lucca, 7-11 May 2018. <https://complexity72h.weebly.com/>

-
- [1] F. Allen and D. Gale, in *The Risks of Financial Institutions* (University of Chicago Press, 2007), pp. 341–376.
 - [2] P. Gai and S. Kapadia, **466**, 2401 (2010).
 - [3] A. G. Haldane and R. M. May, *Nature* **469**, 351 (2011).
 - [4] F. Allen, A. Hryckiewicz, O. Kowalewski, and G. Tümer-Alkan, *Journal of Financial Stability* **15**, 112 (2014).
 - [5] D. Acemoglu, A. Ozdaglar, and A. Tahbaz-Salehi, *American Economic Review* **105**, 564 (2015).
 - [6] H. Amini, R. Cont, and A. Minca, *Mathematical Finance* **26**, 329 (2016).
 - [7] S. Battiston, J. D. Farmer, A. Flache, D. Garlaschelli, A. G. Haldane, H. Heesterbeek, C. Hommes, C. Jaeger, R. May, and M. Scheffer, *Science* **351**, 818 (2016).
 - [8] M. Boss, H. Elsinger, M. Summer, and S. Thurner, *Quantitative Finance* **4**, 677 (2004).
 - [9] E. W. Nier, J. Yang, T. Yorulmazer, and A. Alentorn, *Journal of Economic Dynamics and Control* **31**, 2033 (2007).
 - [10] J. F. Cocco, F. J. Gomes, and N. C. Martins, *Journal of Financial Intermediation* **18**, 24 (2009).
 - [11] C.-P. Georg, *Journal of Banking and Finance* **37**, 2216 (2013).
 - [12] A.-C. Hüser, *Journal of Network Theory In Finance* **1**, 1 (2015).
 - [13] P. Barucca, M. Bardoscia, F. Caccioli, M. D’Errico, G. Visentin, S. Battiston, and G. Caldarelli, *Network valuation in financial systems*, <https://arxiv.org/abs/1606.05164> (2016).
 - [14] L. Eisenberg and T. H. Noe, *Management Science* **47**, 236 (2001).
 - [15] C. Furfine, *Journal of Money, Credit, and Banking* **35**, 111 (2003).
 - [16] S. Battiston, M. Puliga, R. Kaushik, P. Tasca, and G. Caldarelli, *Scientific Reports* **2**, 541 (2012).
 - [17] S. Thurner and S. Poledna, *Scientific Reports* **3**, 1888 (2013).
 - [18] I. Mastromatteo, E. Zarinelli, and M. Marsili, *Journal of Statistical Mechanics: Theory and Experiment* **2012**, P03011 (2012).
 - [19] T. Roukny, H. Bersini, H. Pirotte, G. Caldarelli, and S. Battiston, *Scientific Reports* **3**, 2759 (2013).
 - [20] C. León and R. J. Berndsen, *Journal of Financial Stability* **15**, 241 (2014).
 - [21] M. Montagna and T. Lux, *Quantitative Finance* **17**, 101 (2017).
 - [22] M. Bardoscia, S. Battiston, F. Caccioli, and G. Caldarelli, *Nature Communications* **8**, 14416 (2017).
 - [23] S. Battiston, G. Caldarelli, M. D’Errico, and S. Gurciullo, *Statistics & Risk Modeling* **33**, 117 (2016).
 - [24] P. Angelini, A. Nobili, and C. Picillo, *Journal of Money, Credit and Banking* **43**, 923 (2011).
 - [25] K. Anand, I. van Lelyveld, A. Banai, T. Christiano Silva, S. Friedrich, R. Garratt, G. Halaj, I. Hansen,

- B. Howell, H. Lee, et al., *Journal of Financial Stability* **35**, 107 (2018).
- [26] G. Cimini, T. Squartini, D. Garlaschelli, and A. Gabrielli, *Scientific Reports* **5**, 15758 (2015).
- [27] J. Park and M. E. J. Newman, *Physical Review E* **70**, 066117 (2004).
- [28] T. Squartini and D. Garlaschelli, *New Journal of Physics* **13**, 083001 (2011).
- [29] G. Caldarelli, A. Capocci, P. De Los Rios, and M. A. Muñoz, *Physical Review Letters* **89**, 258702 (2002).
- [30] G. Cimini, T. Squartini, A. Gabrielli, and D. Garlaschelli, *Physical Review E* **92**, 040802 (2015).
- [31] T. Squartini, G. Cimini, A. Gabrielli, and D. Garlaschelli, *Applied Network Science* **2**, 3 (2017).
- [32] M. Bardoscia, S. Battiston, F. Caccioli, and G. Caldarelli, *PLoS ONE* **10**, e0130406 (2015).
- [33] M. Bardoscia, F. Caccioli, J. I. Perotti, G. Vivaldo, and G. Caldarelli, *PLoS ONE* **11**, e0163825 (2016).